Mathematical modelling to reduce animal use in neurodevelopmental safety assessment in humans

Richard Currie (problem presenter),
John Chapman, Louise Dyson, Morgan Germain, Beth McMillan,
Dennis Reddyhoff, Daniel Temko, John Ward and Steven Webb

January 21, 2016

Abstract

There is increasing regulatory interest in the potential for chemicals to adversely affect neuronal development via perturbations of the thyroid hormone signalling system. It is known that in adult rodents this system can be perturbed through induction of uridine 5'-diphospho-glucuronosyltransferases (UGT), which is likely to occur in approximately 1/3 of crop protection chemicals. However the effects in developing rodents have not been as extensively studied as in adults. This has led to a requirement to conduct developmental thyroid studies to assess the potential for adverse effects via UGT induction. As each of these studies uses approximately 2000 rats, meeting this knowledge need may require large numbers of animals. By modelling the thyroid hormone metabolic and signalling pathways we aim to provide information that can be used to inform safety assessments with minimal need to perform additional developmental thyroid studies. Specifically we want to know whether we can simulate the effect of increased T4/T3 metabolism in the liver on plasma T3/T4 levels and the consequence of this on thyroid hormone concentrations and signalling in the developing foetal brain through gestation and lactation.

We have formulated a mechanistic model of the requisite chemical reactions and feedbacks for thyroid hormone signalling in the brain, and simulated this model in two ways. Firstly we use a Petri Net simulation of the model, which creates a stochastic simulation of the considered network, with the assumption that all the reaction rates are equal. Using this simulation we show that T3 inhibition is not the limiting factor in the production of D2 and that removing ubiquitinylation has a large effect on T4 concentrations and increases the total amount of D2 in the system. Secondly, we consider the system deterministically, using a system of ordinary differential equations (ODEs). This model can be solved numerically and, under reasonable assumptions, analytically at steady state. We demonstrate that this model displays homeostasis in some parameter regimes, in the sense that levels of T3 do not change dramatically with changing levels of T4e. We also discuss the relative importance of two different homeostatic mechanisms within the system. Finally we discuss ways of incorporating this model into a pharmacokinetic model to discover how thyroid signalling in the brain may affect hormone concentrations in other parts of the body, and how perturbations to maternal thyroid signalling may affect hormone concentrations in a developing foetal brain.

1 Introduction and problem description

All pharmaceutical and crop protection and some environmental pollutants and industrial chemicals go through a battery of tests, many of which involve animals, to assess their potential for inducing adverse effects in humans and the environment. A common finding during these investigations is the induction of Phase II xenobiotic metabolism in rats [1]. This results in increased thyroid hormone metabolism.

Thyroid hormones are essential for the control of metabolism and development, especially nervous system development. Therefore there is a concern that altered thyroid hormone levels during critical periods of development would result in adverse outcomes in the developing foetus. This has led to calls from the regulatory agencies, e.g. the US Environmental Protection Agency (US EPA) to perform additional "developmental thyroid" studies in rats to assess the risk to the foetus and infants.

Thyroid hormone homeostasis is maintained through a negative feedback system involving the hypothalamus, pituitary and thyroid glands (HPT axis) as shown in Figure 1. In humans, the free concentration of the thyroid hormones thyroxine (T4) and triiodothyronine (T3) are low because they are mostly bound to thyroxine-binding globulin, transthyretin or albumin. Rats do not have thyroxine-binding globulins and consequently free concentrations are higher, metabolism is faster and the thyroid system is more active than humans, making them less than ideal models for studying human thyroid hormone-dependent developmental toxicities.

T4 and T3 can cross cell membranes, however they can also be transported across the blood-brain barrier via transport proteins [2]. T3 is the active hormone that binds to thyroid hormone receptors, which then alters gene expression and so produce a biological response. Most T3 is produced intracellularly from T4 by the action of the D2 deiodinase. The D2 deiodinase is regulated by ubiquination, which is stimulated by the substrate, T4. T4/T3 acts on the pituitary gland and hypothalamus to negatively regulate the production of thyroid stimulating hormone

(TSH) and thyrotropin releasing hormone, respectively; hormones essential for the synthesis and secretion of T4 and T3 from the thyroid gland. T3 and T4 can be metabolised to inactive forms by D1 and D3 deiodinases and can also be conjugated by a number of uridine 5'-diphospho-glucuronosyltransferases (UGTs) and sulfotransferases (SULTs) to increase clearance from the liver into the bile.

One of the most frequently observed effects in safety testing of chemicals is induction of xenobiotic metabolism systems in the liver. This adaptive response to a chemical permits the clearance of that chemical. However it also increases the expression of T3 and T4 UGTs, for example see [3]. In the male rat this results in decreased T3/T4 levels, increased TSH, prolonged proliferative stimulation of the thyroid and benign tumours. These tumours are known not to be relevant for humans due to differences in response in the human HPT axis to decreased T3/4, compared to the rodent. Standard practice would be to demonstrate the perturbation of thyroid hormone levels using a variety of doses and establish a no-effect level dose where no perturbations in thyroid hormone levels are observed.

Human data show that maternal thyroid hormones are necessary for early foetal neurodevelopment and that normalisation of maternal thyroid T4 levels when in a hypothyroid state is required to prevent mental retardation in children [4, 5]. Once the foetal thyroid is able to produce thyroid hormones, there is a shift so that the maternal supply of thyroid hormones is quantitatively less important.

Therefore to adequately assess the risk to human neurodevelopment caused by chemicals that induce UGT enzymes in the liver, a model will have to integrate many things (1) the intracellular negative feedback regulation of the deiodinases; (2) the negative feedback regulation controlling thyroid hormone secretion at the organism level, (3) kinetics and metabolism in two nested compartments (the mother and foetus in placenta), (4) extrapolate across changing expression of key components of the system at different life stages and (5) extrapolate across species from the data that is available.

1.1 Impact on medicine and healthcare

The modelling will cover key developmental stages when critical neurodevelopmental effects of thyroid hormones are occurring. In many parts of the world hypothyroidism (whether through thyroid disease or iodine deficiency) contributes to childhood neurological impairments [5, 6], understanding whether UGT induction caused by pharmaceuticals or trace environmental chemicals is able to exacerbate these effects has implications both for clinical practice and public health.

1.2 Impact on Animal Use

The design of developmental thyroid studies under the USEPA guideline [7] would involve testing in the region of 2000 rats per study (the exact number depends on the number of dose groups and the litter size of the strain used). This estimate does not include any that might be required for a preliminary study to ensure appropriate dose level selection. Approximately one third of Syngenta's existing crop protection chemicals have some form of liver effect that is likely to include UGT induction and so we can estimate an upper limit of 40000 animals for this one company alone. Consequently if the modelling is useful in permitting a reliable extrapolation from adult rats to effects in humans, then the need to conduct these studies to meet this knowledge need may be eliminated or reduced with the consequent reduction in projected animal usage.

1.3 Questions to be answered

Can you simulate the effect of increased T4/T3 metabolism in the liver on plasma T3/T4 levels and the consequence of this on thyroid hormone concentrations and signalling in the developing foetal brain through gestation and lactation? Can you extrapolate the thyroid hormone dose response observed in the male rat to the human foetus and neonate and examine the potential for interaction with established risk factors for hypothyroidism such as iodine deficiency.

2 Modelling

We formulate a mechanistic model of the chemical reaction network in brain cells. The model is shown diagrammatically in Figure 1. The model can be described in the following way. External T4 (T_{4e}) enters the cell and is turned into T3 in a reaction that is catalysed by D2. This is regulated by the ubiquitination of the T4D2 complex, which marking the complex for degradation. In turn, T3 downregulates the production of D2. In other cells close by D3 catalyses the production of rT3 from T4 and T2 from T3, while D2 can also catalyse the change of rT3 into T2. Since the two types of cells are very close and are of approximately the same size, we assume that all reactions occur together, and do not explicitly include the movement of T2, rT3, T3 and T4 between the two types of cells.

To model the downregulation by T3 of the production of D2, we explicitly include the binding of T3 to receptors (R) on the DNA to form bound DNA (DNA_B). Meanwhile the fraction of the total amount of DNA (DNA_T) that is free (DNA_F) produces mRNA (m), which in turn gives D2. Using the conservation of receptors (so that $R = R_0 - [T_3R]$), and of DNA (so that $DNA_B = DNA_T - DNA_F$), we write down the following system of ordinary differential equations

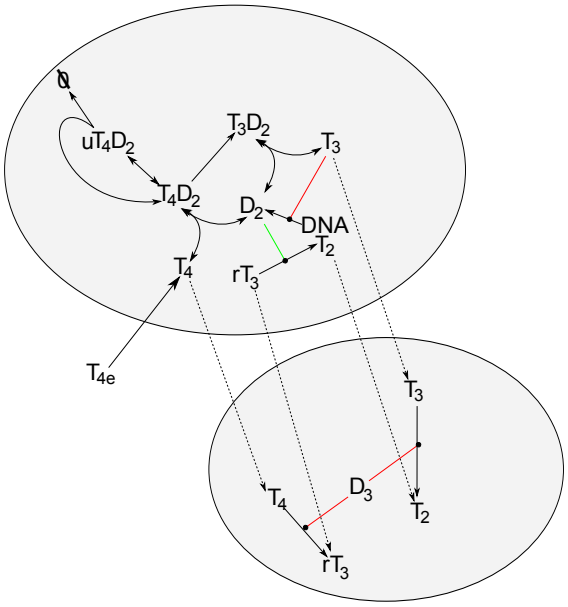

Figure 1: Diagram of the modelled reaction network

(ODEs), using mass action kinetics, with Michaelis Menten terms for catalysed reactions:

$$\frac{\mathrm{d}T_4}{\mathrm{d}t} = k_3(T_{4e} - T_4) - k_4 T_4 D_2 + k_{-4}[T_4D_2] + k_5[uT_4D_2] - \frac{k_6 D_3 T_4}{k_7 + T_4}, \quad (1)$$

$$\frac{\mathrm{d}T_3}{\mathrm{d}t} = k_8[T_3D_2] - \frac{k_9 D_3 T_3}{k_{10} + T_3} - k_{11}(T_3 - T_{3e}), \quad (2)$$

$$\frac{\mathrm{d}D_2}{\mathrm{d}t} = k_{16}m - k_{17}D_2 - k_4 T4 D_2 + k_{-4}[T_4D_2] + k_8[T_3D_2], \quad (3)$$

$$\frac{\mathrm{d}[T_4D_2]}{\mathrm{d}t} = -k_{18}u[T_4D_2] + k_{19}[uT_4D_2] - k_{20}[T_4D_2] + k_4 T4 D_2 - k_{-4}[T_4D_2], \quad (4)$$

$$\frac{\mathrm{d}[T_3D_2]}{\mathrm{d}t} = k_{20}[T_4D_2] - k_8[T_3D_2], \quad (5)$$

$$\frac{\mathrm{d}[uT_4D_2]}{\mathrm{d}t} = k_{18}u[T_4D_2] - k_{19}[uT_4D_2] - k_5[uT_4D_2], \quad (6)$$

$$\frac{\mathrm{d}[T_3R]}{\mathrm{d}t} = a_1 T_3(R_0 - [T_3R]) - a_{-1}[T_3R] - a_2[T_3R]DNA_F + a_{-2}(DNA_T - DNA_F), \quad (7)$$

$$\frac{\mathrm{d}[DNA_F]}{\mathrm{d}t} = -a_2[T_3R]DNA_F + a_{-2}(DNA_T - DNA_F), \quad (8)$$

$$\frac{\mathrm{d}m}{\mathrm{d}t} = a_3\frac{DNA_F}{DNA_T} - a_4 m, \quad (9)$$

$$\frac{\mathrm{d}T_{3e}}{\mathrm{d}t} = k_{11}(T_3 - T_{3e}), \quad (10)$$

where complexes are denoted in square brackets and $[uT_4D_2]$ is the ubiquitinated complex $[T_4D2]$.

3 Petri Net

We constructed a Petri net based on the equations above, using the assumption that the rate constants were all set to 1. The structure is shown in Figure 2. Highlighted in pink are the two concentrations that we modified in our analysis: the extracellular T4 concentration (T4e) and the concentration of receptor inside the nucleus (R). Highlighted in blue are the two concentrations that were set to values higher than 0, namely the intracellular D2 concentration, and the concentration of free DNA that codes for the D2 enzyme. Highlighted in yellow is the concentration that we were interested in measuring: the concentration of receptor-bound T3.

In our analysis, we aimed to answer four questions:

1. How does the initial extracellular T4 supply affect the steady-state T3R concentration?
2. What happens if we remove the ubiquitinylation of the T4D2 complex from the network?
3. What happens if we remove T3's inhibitory effect on D2 production?
4. What if we remove both of these features?

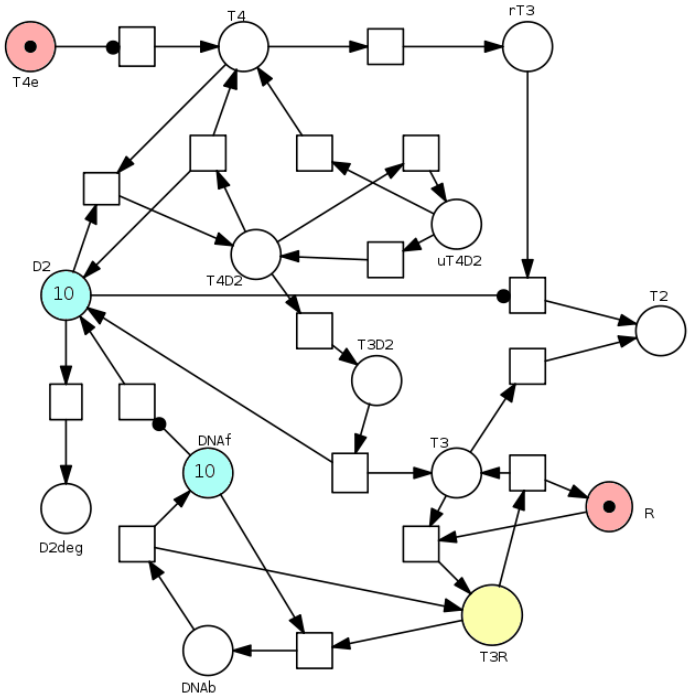

Figure 2: Structure of the Petri net. The Petri Net consists of two types of nodes, places (represented by circles) and transitions (represented by squares). Places correspond to proteins such as enzymes and receptors, tokens (represented by dots or numbers inside a place) can be assigned to each place to represent the relative quantity of the particular protein, for example as a measurement of concentration or amount fo protein. Interactions, such as binding and activation, between these proteins are represented by transitions. Places and transitions are connected by weighted, directed edges/arcs (represented by arrows). Firing of a transition transfers tokens from preplaces to postplaces.

The model used to answer the first question (Q1) is shown in Figure 2. The remaining three questions (Q2-Q4) were explored using modifications of this Petri net, with the appropriate places and transitions removed.

We used stochastic simulations to find out the effects of different molecules on the steady state concentrations of other molecules.

3.1 Results

Figure 3 shows a typical time course for the Q1 model. The concentrations of each molecule in the net quickly reached a steady state in each simulation.

Figure 4a shows the concentration of receptor-bound T3 that results from increasing concentrations of extracellular T4 while the concentration of receptor is high. The four lines correspond to each of the four questions under investigation. Removing ubiquitinylation (Q2) reduced the amount of T3R, while removing T3 inhibition (Q3) greatly increased T3R concentration, and the combination of these two removals (Q4) had an effect somewhere inbetween. The large discontinuity at initial T4e concentrations of 10 is caused by the initial seeding of 10 tokens for D2 and DNAf - different initial seedings created similar discontinuities. Figure 4b shows the same graph for a larger range of initial T4e concentrations. The same trend in differences between models can be observed. The T3R concentrations reach a plateau when the initial T4e concentration is increased to 100. The final height of these plateaus was determined by the initial concentration of R (data not shown), which can be considered to be abundant.

The amount of total T4 (the sum of free T4, extracellular T4, and enzyme-bound T4, but not the ubiquitinylated T4 complex) is shown in Figure 4c. The T4 concentration in Q2 is identical to that in the unaltered model, indicating that reduced inhibition of D2 synthesis does not increase the total amount of T4 in the system. However, Figure 4d shows the total D2 concentration in the model, and the concentration in Q1 is not increased from the full model. This indicates that T3 inhibition is not the limiting factor in D2 production under these conditions.

The T4 concentrations in Q3 and Q4 (as shown in Figure 4c) show that removing ubiquitinylation has a large effect on T4 concentration, and also increases the amount of total D2 in the system, as can be expected, because the removal of this step prevents the degradation of the T4D2 complex.

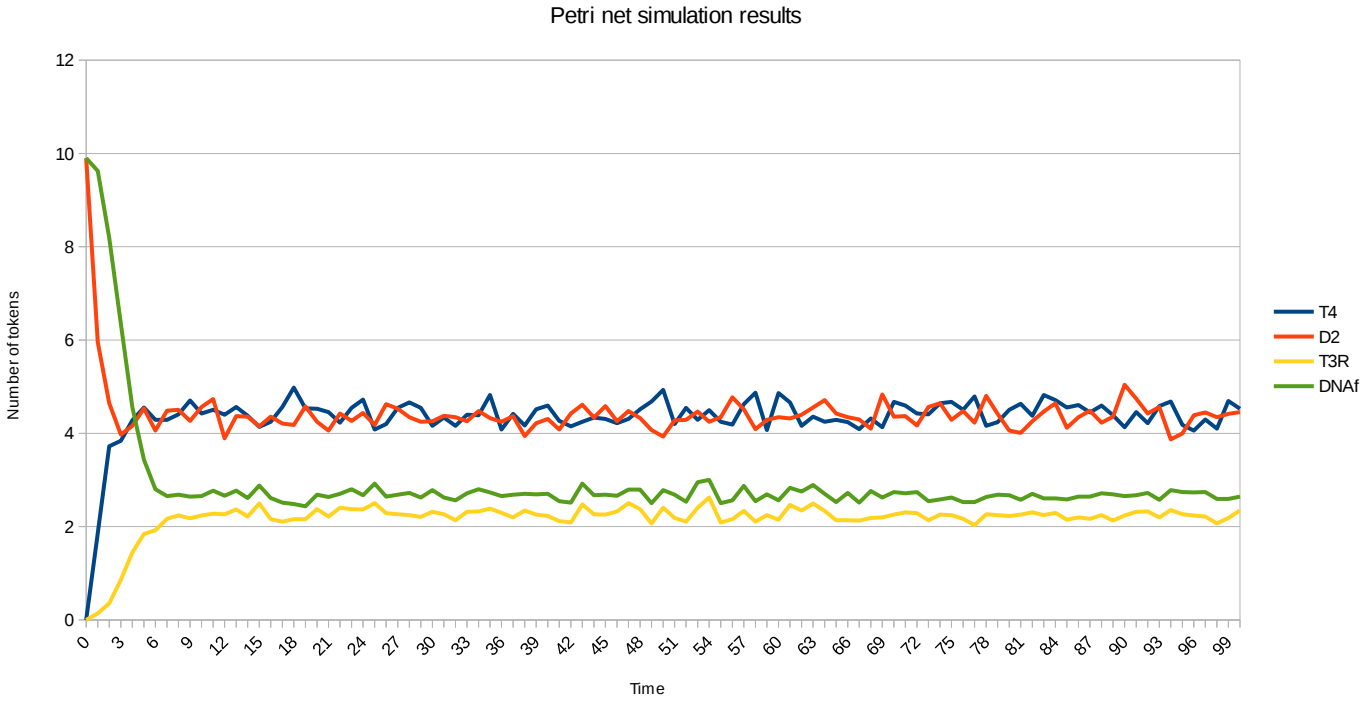

Figure 3: An example of the concentrations of key molecules over the course of the petri net stochastic simulation. Time is defined as the number of steps the simulation has taken, and the number of tokens at each place in the net correspond to the concentration of those molecules. The system quickly reaches a steady state.

4 Numerical solutions

We may solve the model equations (Eqns (1)–(10)) numerically using Matlab's ode15s. We take the following order of magnitude approximations to the parameters such that binding reactions are fast and small molecule-protein binding reactions are faster than macromolecular interactions:

$$\begin{array}{lllllll} k_3 = 1, & k_4 = 100, & k_{-4} = 10, & k_5 = 1, & k_6 = 1, & k_7 = 1, & k_8 = 100, \\ k_9 = 1, & k_{10} = 1, & k_{11} = 1, & k_{12} = 1, & k_{13} = 1, & k_{14} = 1, & k_{15} = 1, \\ k_{16} = 1, & k_{17} = 1, & k_{18} = 10, & k_{19} = 1, & k_{20} = 10, & a_1 = 100, & a_{-1} = 1, \\ a_2 = 10, & a_{-2} = 0.1, & DNA_T = 1, & a_3 = 1, & a_4 = 1, & D_3 = 1, & u = 1, \\ R_0 = 1, & T_4e = 1, & & & & & \end{array} \tag{11}$$

and assume that all variables are initially zero. Numerical solutions (Figure 5) reveal an initial transient followed by steady state values. T_4 and T_3 are high compared to the other variables in this parameter regime, and all variables except for T_3 show initially higher transients, followed by lower steady state values.

5 Steady state solutions

We wish to investigate the effect of a change in external T_4 (T_4e) on the concentrations of receptor-bound T_3, and discover how this depends on the different homeostatic mechanisms in the system. Since we assume that the initial dynamic transient may be quick, we will look for steady state solutions, in which we can explicitly see the dependence on different parts of the system.

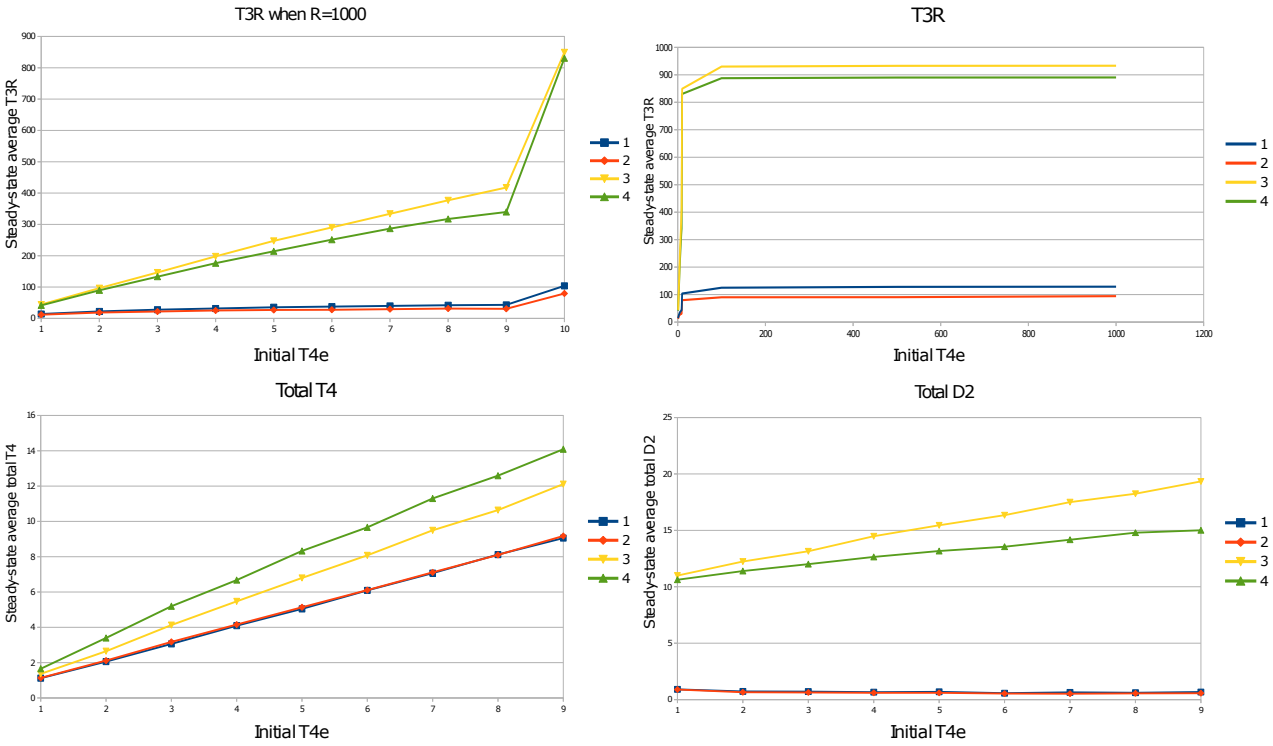

Figure 4: PetriNet simulations exploring the four questions in Section 3. In each figure the lines 1-4 correspond to each of the four questions, while the subgraphs plot different quantities as the initial level of extracellular T_4 varies.

To solve the system at steady state, we set Eqns (1)–(10) equal to zero. Solving Eqns (2)–(10) simultaneously in terms of T_3 and substituting into Eq. (1) reduces the problem to the solution of a quintic in T_3. Unfortunately the solution to this is very difficult to find. However, if we assume that $T_4 \ll k_7$ and $T_3 \ll k_{10}$ (as seems somewhat reasonable, given the numerical solutions) then

$$\frac{k_6 D_3 T_4}{k_7 + T_4} \approx \frac{k_6}{k_7} D_3 T_4, \tag{12}$$

$$\frac{k_9 D_3 T_3}{k_{10} + T_3} \approx \frac{k_9}{k_{10}} D_3 T_3, \tag{13}$$

and the order of the equation is much lower and can be solved exactly. The problem then reduces to the solution to the cubic equation

$$\begin{aligned}
&a_1 a_4 D_3^2 k_{18} k_4 k_5 k_9^2 u(a_{-2} + a_2 R_0)\ T_3^3 \\
-\Big[&a_1 a_3 a_{-2} D_3 k_{16} k_{20} k_4 (k_{19} + k_5) k_9 - a_4 a_{-1} a_{-2} D_3^2 k_{18} k_4 k_5 k_9^2 u + a_1 a_4 D_3 k_{18} k_3 k_4 k_5 k_9 u(a_{-2} + a_2 R_0) T_4 e \\
&+ a_1 a_4 D_3 k_1 7 (k_3 + D_3 k_6) k_9 (a_{-2} + a_2 R_0)((k_{19} + k_5)(k_{20} + k_{-4}) + k_{18} k_5 u)\Big]\ T_3^2 \\
-\Big[&a_3 a_{-1} a_{-2} D_3 k_{16} k_{20} k_4 (k_{19} + k_5) k_9 - a_1 a_3 a_{-2} k_{16} k_{20} k_3 k_4 (k_{19} + k_5) T_4 e \\
&+ a_4 a_{-1} a_{-2} D_3 k_{18} k_3 k_4 k_5 k_9 T_4 e u + a_4 a_{-1} a_{-2} D_3 k_1 7 (k_3 + D_3 k_6) k_9 ((k_{19} + k_5)(k_{20} + k_{-4}) + k_{18} k_5 u)\Big]\ T_3 \\
&+ a_3 a_{-1} a_{-2} k_{16} k_{20} k_3 k_4 \Big[k_{19} + k_5\Big] T_4 e = 0,
\end{aligned} \tag{14}$$

which may be solved using the formula for the roots of a cubic equation. We use the same order of magnitude parameter values as in Section 4. This gives three solutions: one that is always negative; one that gives a negative values for D_2 and T_4; and a third, biologically realistic, solution. Keeping $T_4 e$ as a variable input, this gives

$$\begin{aligned}
T_3 = {} & 0.04 + (1.3 \times 10^{-7} + 2.27 \times 10^{-7} i) A + \frac{T_4 e}{3} \\
& + \frac{(3271.24 - 5492.75i) + T_4 e((38238.6 - 66231.2i) + (212087. - 367345.i) T_4 e)}{A}
\end{aligned} \tag{15}$$

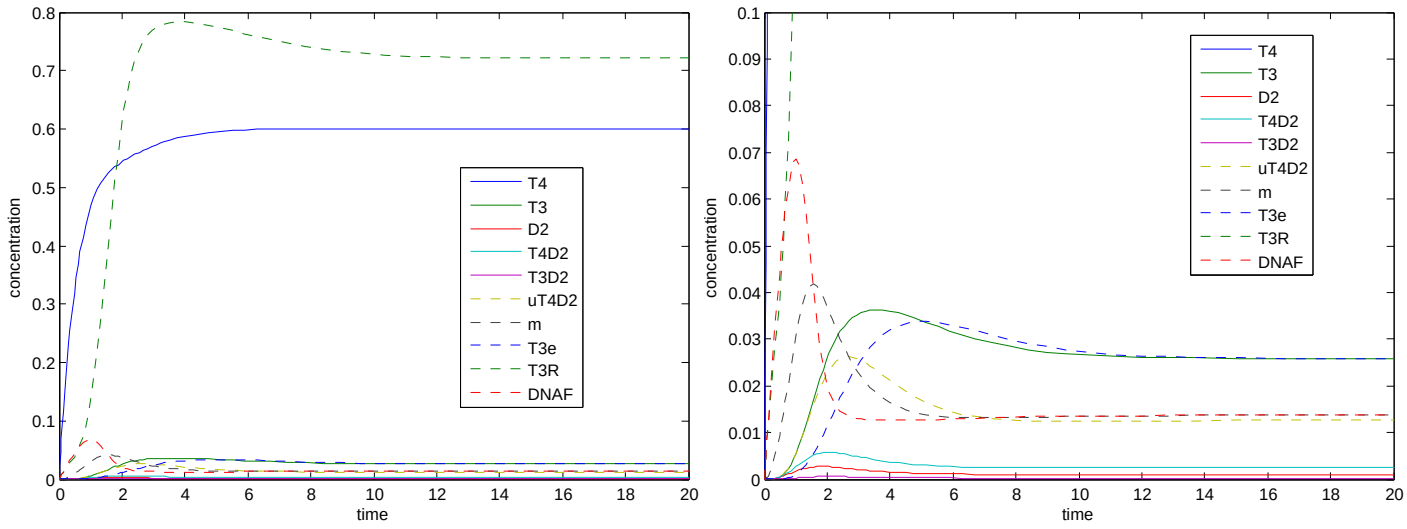

Figure 5: Numerical solutions to the model

where

$$A = (-3.76513 \times 10^{15} - 6.31276 \times 10^{16} T_4e - 5.57281 \times 10^{17} T_4e^2 - 2.0606 \times 10^{18} T_4e^3 \tag{16}$$

$$+ i\sqrt{1.87846 \times 10^{28} + 3.81196 \times 10^{31} T_4e + 8.58035 \times 10^{32} T_4e^2 + 7.69161 \times 10^{33} T_4e^3 + 3.38282 \times 10^{34} T_4e^4})^{1/3}. \tag{17}$$

Note that this may in principle be complex. However a given cubic equation,

$$ax^3 + bx^2 + cx + d = 0, \tag{18}$$

has three real roots if

$$\Delta = 18abcd - 4b^3d + b^2c^2 - 4ac^3 - 27a^2d^2 > 0. \tag{19}$$

For Eq. 14

$$\Delta = 6.82 \times 10^{14} + 1.38 \times 10^{18} T_4e + 3.12 \times 10^{19} T_4e^2 + 2.79 \times 10^{20} T_4e^3 + 1.23 \times 10^{21} T_4e^4, \tag{20}$$

and thus $\Delta > 0$ for all $T_4e > 0$, so that all the roots of Eq. 14 must be real.

5.1 Plotting the steady state solution

Eq. (15) displays the potential for homeostasis against changes in T_4e. As we can see from Figure 6(a), for large enough wildtype levels of T_4e, the curve changes slowly with changing values of T_4e. Hence the levels of T_3 are robust to reducing levels of T_4e. However, if wildtype values are closer to zero, or the reduction in T_4e is too severe, then we may 'fall off' the flatter part of this curve, and may see catastrophic reactions to changes in T_4e. Thus the robustness of the system to varying concentrations of T_4e depend on the exact parameter values *in vivo* and the initial, wildtype levels of T_4e.

Since the functional effect of changing T_4e levels is effected by the binding of T_3 to receptors in the nucleus, we also plot this against T_4e (Figure 6(b)) and note that the shape of the curve is in fact more definitely separated into a homeostatic regime (for T_4e greater than about 0.5) and a non-homeostatic regime (for $T_4e < 0.5$).

5.2 Assessing the importance of different homeostatic mechanisms

The reaction network has two mechanisms that may help to maintain homeostasis. The first is the ubiquitination, and subsequent removal, of the $[T_4D_2]$ complex, which prevents T_4e from driving large amounts of this complex, which then converts the T_4 into the end product, T_3. Even if T_4e increases by a large amount, this mechanism suppresses the corresponding increase in T_3. The second mechanism is the negative feedback loop whereby T_3 reduces the production of D_2, which in turn catalyses the production of T_3. Thus large levels of T_3 reduce the production of greater amounts of T_3.

We may assess the relative importance of these two mechanisms by switching off each in turn. Setting $k_{18} = k_{19} = 0$ removes the ubiquitination part of the network, and we may then plot the same quantities with the other parameters unchanged. This has a large effect on the T_3 response curve (Figure 6(c)), which is now approximately linear, given by

$$9.92 \times 10^{-6}(-104 + 10000 T_4e + \sqrt{(104 - 10000 T_4e)^2 + 2.02 \times 10^7 T_4e}). \tag{21}$$

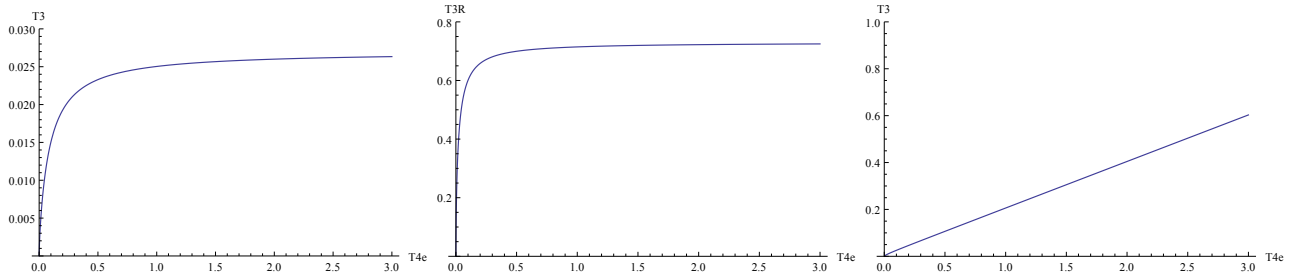

(a) T_3 against T_4e (b) T_3R against T_4e (c) T_3 response to T_4e without ubiquitination

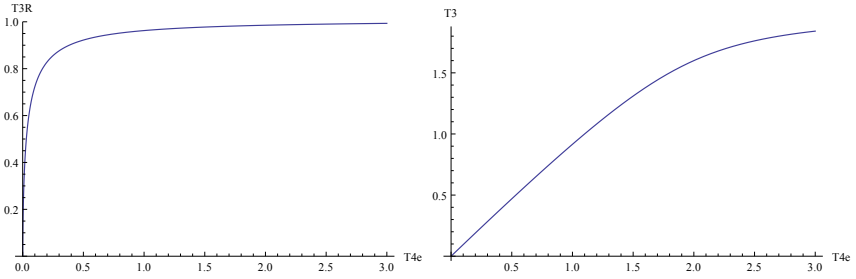

(d) T_3R response to T_4e without ubiquitination (e) T_3 response to T_4e without T_3 DNA regulation

Figure 6: Showing the steady state value of T_3 and receptor bound T_3 as T_4e changes under different conditions

In contrast, removing the regulation of D_2 by T_3 by setting $a_1 = 0$ preserves the general shape of the T_3 (Figure 6(e)), but shifts the curve so that much higher levels of T_4e are required for the system to be homeostatic to changes in T_4e.

In spite of this, the T_3R response curve is relatively unchanged for non-ubiquitination (Figure 6(d)). This is because the dependence of T_3R on T_3 itself provides a homeostatic mechanism. T_3R can be found in terms of T_3 at steady state:

$$T_3R = \frac{a_1 R_0 T_3}{a_{-1} + a_1 T_3}, \tag{22}$$

and is shown in Figure 7. This therefore provides a third homeostatic mechanism, which depends on the relative sizes of a_{-1} and a_1. In essence this mechanism is due to the availability of receptors for T_3, since if all the receptors are already bound by T_3 molecules then further increasing the amount of T_3 has no further effect.

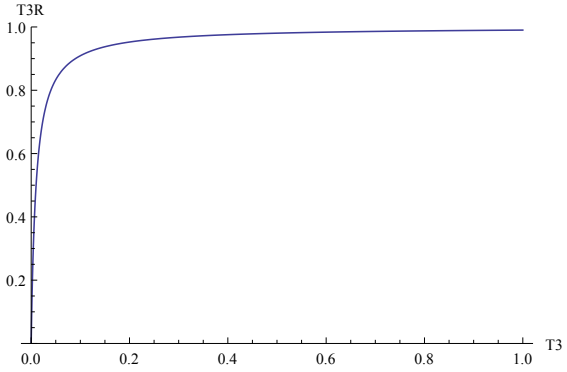

Figure 7: The dependence of T_3R on T_3 at steady state

6 Future work: PK Modelling

6.1 About PK Modelling

Pharmacokinetic or PK modelling explores the transport of drugs through different areas of the body which are modelled as compartments and look at the absorption, distribution, metabolism and excretion of the compound being examined. An example of the major processes involved in drug transport can be found in Figure 2. PK models allow us

to explore the kinetics of T3/T4 interaction throughout the body of a rat or human and observe how these hormones are distributed and absorbed in the different areas of interest.

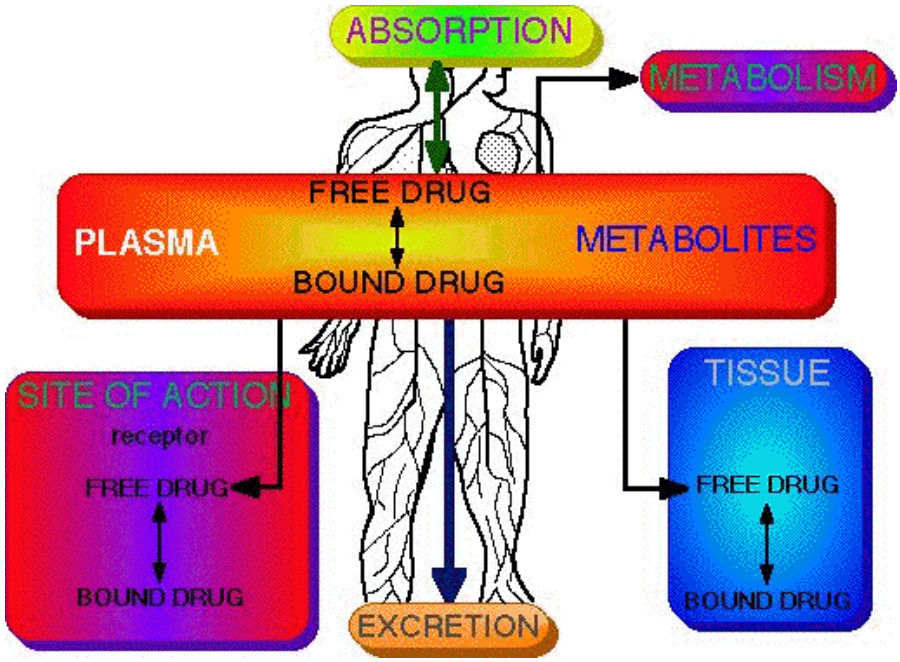

Figure 8: A diagram showing the major processes involved in drug transport. Source: www.booomer.org

6.2 Existing PK models

The two most recent PK models of T3 and T4 metabolism are Eisenberg et al. (2008) and McLanahan et al. (2008). Eisenberg et al. have created a multi compartment model that aims to link the brain and thyroid together. They model the H-P-T axis as a series of fast and slow compartments and use simple transport between this and the brain submodel to monitor T3 and T4 levels over time. This model is a good starting point for our work however the lack of a liver compartment makes the model unsuitable for our desired outcomes, but can be used as a starting point for future PK modelling. McLanahan et al. modelled the distribution of iodide, TSH, T3 and T4 throughout the body as 4 separate compartments each with their own volume of distribution and also included liver blood and tissue compartments for each of the hormones. The work carried out by them provides a good basis for our model and will help us parameterise any PK model we produce.

6.3 Combining PK models with mechanistic models

Over the course of the study group we have created a mechanistic model describing the evolution of T3 and T4 over time in the brain. In the model T4 is transported into the brain cells form an external pool $T4_e$. By having the brain as a compartment in our PK model we will be able to model the change in extracellular T4 and use this to link our PK and mechanistic model. We also must include a compartment for the liver so that we can look at how the change in liver activity of a newborn animal affects T3 levels in the brain. Figure 3 is an example of the different compartments that need to be modelled in order to explore changes in T3 and T4. By selectively using different compartments in this model we can explore the mother-foetus relationship over time and also look at how the physiological changes in a newborn animal change brain T4 and T3 levels.

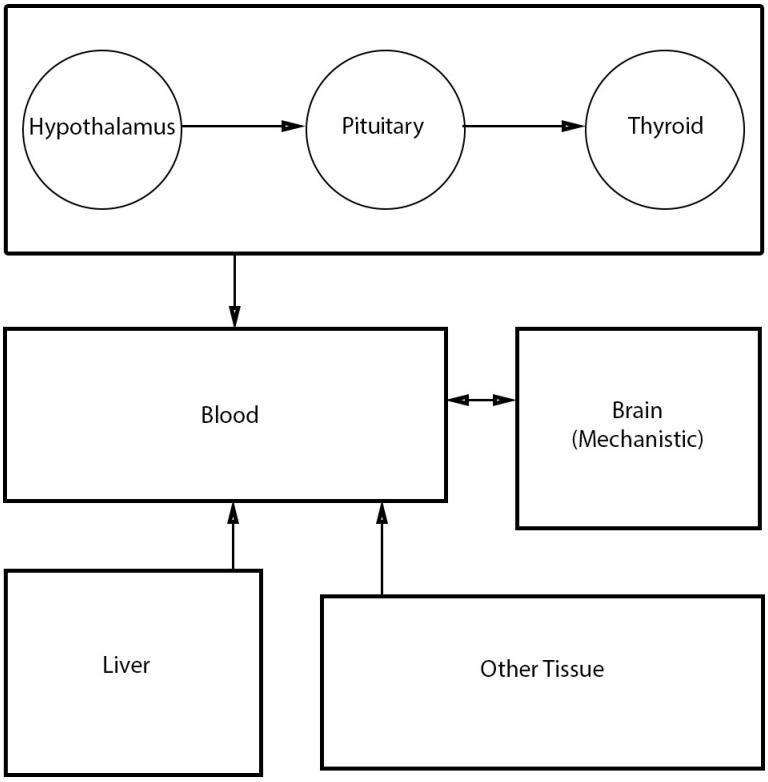

Figure 9: A diagram of our proposed PK model

References

[1] Crofton KM, Zoeller RT. Mode of action: neurotoxicity induced by thyroid hormone disruption during development–hearing loss resulting from exposure to PHAHs. Crit Rev Toxicol. 2005;35(8-9):757–769.

[2] Morte B, Bernal J. Thyroid hormone action: Astrocyte-neuron communication. Front Endocrinol (Lausanne). 2014;5(MAY):2–6.

[3] Paul KB, Hedge JM, DeVito MJ, Crofton KM. Short-term exposure to triclosan decreases thyroxine in vivo via upregulation of hepatic catabolism in Young Long-Evans rats. Toxicol Sci. 2010;113(2):367–79.

[4] Ng L, Hernandez A, He W, Ren T, Srinivas M, Ma M, et al. A protective role for type 3 deiodinase, a thyroid hormone-inactivating enzyme, in cochlear development and auditory function. Endocrinology;(4):1952–60.

[5] DeLong GR, Stanbury JB, Fierro-Benitez R. Neurological signs in congenital iodine-deficiency disorder (endemic cretinism). Developmental Medicine & Child Neurology. 1985;27(3):317–324.

[6] Goldey ES, Kehn LS, Lau C, Rehnberg GL, Crofton KM. Developmental exposure to polychlorinated biphenyls (Aroclor 1254) reduces circulating thyroid hormone concentrations and causes hearing deficits in rats. Toxicol Appl Pharmacol. 1995;135(1):77–88.

[7] Office of Pesticide Programs WD Health Effects Division. Guidance for Thyroid Assays in Pregnant Animals, Fetuses and Postnatal Animals, and Adult Animals; 2005. [Online; accessed 21-January-2016]. `http://www.epa.gov/sites/production/files/2015-06/documents/thyroid_guidance_assay.pdf`.